

The development of a continuous isothermal titration calorimetric method for equilibrium studies

Natalia Markova and Dan Hallén*

Department of Structural Chemistry, Biovitrum AB, S-112 76 Stockholm, Sweden

Received 7 January 2004

Available online 17 June 2004

Abstract

A continuous isothermal titration calorimetry (cITC) method for microcalorimeters has been developed. The method is based on continuous slow injection of a titrant into the calorimetric vessel. The experimental time for a cITC binding experiment is 12–20 min and the number of data points obtained is on the order of 1000. This gives an advantage over classical isothermal titration calorimetry (ITC) binding experiments that need 60–180 min to generate 20–30 data points. The method was validated using two types of calorimeters, which differ in calorimetric principle, geometry, stirring, and way of delivering the titrant into the calorimetric vessel. Two different experimental systems were used to validate the method: the binding of Ba^{2+} to 18-crown-6 and the binding of cytidine 2'-monophosphate to RNase A. Both systems are used as standard test systems for titration calorimetry. Computer simulations show that the dynamic range for determination of equilibrium constants can be increased by three orders of magnitude compared to that of classical ITC, making it possible to determine high affinities. Simulations also show an improved possibility to elucidate the actual binding model from cITC data. The simulated data demonstrate that cITC makes it easier to discriminate between different thermodynamic binding models due to the higher density of data points obtained from one experiment.

© 2004 Elsevier Inc. All rights reserved.

During the past 30 years the development of microcalorimetric instruments and methods have been essential for the general understanding of binding thermodynamics of biological macromolecules and specific biological systems. The sensitivities of the instruments have made it possible to determine affinities on the order of 10 nM ($K = 10^8 \text{ M}^{-1}$) for 1:1 complexes, provided that the enthalpy of binding is of appropriate magnitude. Thermodynamic data from calorimetric protein binding experiments are now often further analyzed with regard to structural energetics [1–3], where changes in hydration and conformational changes of the proteins can be elucidated. ITC¹ is furthermore a handy tool in various stages of the drug discovery process, such as sorting out the molecular mechanisms of action of a protein–ligand complex and serving as an important technique in the lead optimization process. However,

ITC suffers from the relatively small number of binding experiments that are possible to perform per day. Efforts to speed up the calorimetric response by various means have been made. This has been done either by introducing heaters in the reference vessel to compensate for the heat evolved in the measuring vessel [4–6] or by assigning instrumental time constants and applying Tian's equation to dynamically correct the raw calorimetric signal [7] from a fast stepwise titration. Nothing to improve the experimental procedure has so far been done. In an ITC ligand binding experiment small aliquots of the titrant are added into the calorimetric vessel. The number of titration steps is normally 20–30 and each titration step requires 4–8 min, which means that 60–200 min is needed to complete a titration experiment. The number of data points that can be obtained limits the range of equilibrium constants that can be resolved from the data [6,8,9]. To resolve the equilibrium constant for a stepwise titration the product of the equilibrium constant, K , and titrand concentration in the vessel, C_M , should be $1 \leq KC_M \leq 1000$ [6]. The limiting factor for the equilibrium constant determination is the

* Corresponding author. Fax: +46-8-697-2319.

E-mail addresses: dan.hallen@biovitrum.com, dan.hallen@telia.com (D. Hallén).

¹ Abbreviation used: ITC, isothermal titration calorimetry.

number of data points in the transition part of the binding curve where the change in the degree of binding goes from high to low. To widen the range of attainable equilibrium constants one needs to dramatically increase the number of data points in this part. This can be done by radically decreasing the change in molar ratio (e.g., ligand to protein) between two consecutive additions.

In this work we have explored the possibility of shortening the time of an ITC experiment by slow continuous titration into the calorimetric vessel (cITC). This has to our knowledge not been tried before in connection with microcalorimetric instruments. The idea of adding liquid continuously has earlier been realized for isoperibolic calorimeters [10–12] and Calvet-type calorimeters [13]. These calorimeters are macrocalorimeters where the calorimetric vessels are 25–100 ml and the measured thermal powers are several orders of magnitude larger than those for microcalorimeters. No further developments have been reported on continuous titration after the mentioned works on macrocalorimeters. Here we demonstrate the possibilities of cITC for two different types of microcalorimeters. The calorimeters represent two different types of geometries, stirring arrangements, and measuring principles. We have applied the methodology to systems that have been suggested as calibration and test reactions for titration calorimetry [14,15]. We discuss the benefits of cITC with regard to time of experiments, binding model selection, and the range of attainable equilibrium constants.

Materials and methods

Materials

BaCl₂ · 2H₂O, KAc, and KCl (Fluka) were of the highest grade available. The 18-crown-6 and cytidine 2'-monophosphate obtained from Sigma were 99.9 and 97% pure, respectively. All chemicals were used as received without further purification.

Ribonuclease A from bovine pancreas (EC 3.1.27.5; Fluka), 90% pure, was dialyzed overnight at 4 °C against 1000-fold excess of the buffer (20 mM KAc, 20 mM KCl, pH 5.5). The concentration of RNase A was determined spectrophotometrically at 280 nm using an extinction coefficient of 9440 cm⁻¹ M⁻¹ calculated from the protein composition following the Sednterp program [16].

Calorimetry

In this study we have used two different types of microcalorimeters. They differ in measuring principle, geometries of the calorimetric vessels, stirring, and injection setup.

Type 1 calorimeter. The type 1 calorimeter is a heat-flow twin microcalorimeter with an insertion titration

unit, ThermoMetric 2277 TAM (Thermometric AB, Sweden) [17,18]. The titration unit contains a 1-ml stainless steel cylindrical vessel (can accommodate up to 1.2 ml of solution) equipped with a golden propeller stirrer. The stirring speed is normally adjusted between 60 and 120 rpm.

Titration was performed using a Hamilton syringe mounted onto a computer-controlled pump (Thermometric 6120 Lund Pump) equipped with a step-motor. The titrand is guided into the titration vessel through a stainless steel hypodermic needle permanently attached to the syringe. The tip of the injection needle is positioned 1 mm above the upper part of the propeller stirrer.

In a typical experiment 900 µl of a reactant solution was loaded in the vessel and stirred at 60 or 120 rpm. A nonstirred titration unit charged with 900 µl of water was used on the reference side of the microcalorimeter. The continuous injections were performed using a 250-µl Hamilton syringe. The injection rates ranged from 0.06 to 0.2 µl/s. Electrical calibrations were performed prior to each titration experiment to evaluate the calorimetric gain and the time constants of the instrument. These parameters were further validated in a chemical steady state calibration.

Type 2 calorimeter. The type 2 calorimeter is an adiabatic heat-compensating microcalorimeter with a fixed-in-place nonremovable cell, MCS ITC unit (Microcal, MA, USA). The calorimeter is equipped with a coin-shaped 1.36-ml total-fill overflow cell made of Hastelloy-C alloy. A twin nonstirred reference cell was filled with water.

Injections were performed through a long needle of a spinning syringe equipped with a step-motor. A paddle-shaped tip of the needle serves as a stirrer. A 100-µl syringe was used at the minimum rate possible (0.135 µl/s). The stirring speed was set to 400 or 700 rpm.

Principles of data evaluation for 1:1 binding model

The thermal power, P , for a cITC 1:1 binding is related to the enthalpy of binding, ΔH , by

$$P = \Delta H \cdot \frac{d([ML])}{dt} \cdot V_i, \quad (1)$$

where P is the thermal power; $[ML]$ denotes the molar concentration of the complex, and V_i is the current volume of the solution in the calorimetric vessel. Eq. (1) can be rewritten with respect to the total concentration of the ligand, $[L_{tot}]$, and the degree of its conversion, α :

$$P = \Delta H \cdot \alpha \cdot \frac{d([L_{tot}])}{dt} \cdot V_i. \quad (2)$$

It was shown by Wiseman et al. [6] that the degree of conversion for the 1:1 binding model can be expressed through the binding/association constant K and the total concentrations of the ligand and the macromolecule $[M_{tot}]$,

$$\alpha = \frac{d([ML])}{d([L_{tot}])} = 0.5 + \frac{1 - (1 + r)/2 - X_r/2}{(X_r^2 - 2X_r(1 - r) + (1 + r)^2)^{0.5}}, \quad (3)$$

where

$$r = 1/(K \cdot [M_{tot}]) \quad \text{and} \quad X_r = [L_{tot}]/[M_{tot}].$$

Note that a correction for the dilution of the reactants must be done for a *type 1 calorimeter*. A combined correction for the dilution and displacement of a part of the reacting mixture from the total-fill calorimetric vessel has to be applied to the *type 2 calorimeter* data [19]. The integral of the thermal power–time curve for the complete cITC experiment provides a first good estimate for the enthalpy of the process:

$$\Delta H \cong \frac{1}{[M_{tot}] \cdot V_f} \int_0^t P dt. \quad (4)$$

A continuous set of the data on the degree of conversion, α , can be directly obtained through Eqs. (2) and (4), providing a good starting point for the data-fitting procedure. The data on the degree of conversion and the total concentrations of the reactants are fitted to Eq. (3).

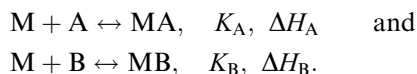
Simulation experiments

We have performed computer simulation experiments to compare the difference in performance between classical ITC and cITC. In the simulation experiments we generated heats for ITC and thermal powers for cITC with added random noise using a competition binding model in which two ligands bind to the same binding site. The generated binding data were fitted to three different binding models, a 1:1 binding model, a competition 1:1 binding model, and a 2:1 binding model.

Competitive binding of two different ligands

The procedure for evaluating equilibrium constants and enthalpies from ITC data for competition experiments has earlier been described in detail by Sigurskjöld [19]. Here we outline the data treatment for cITC.

To describe the equilibrium concentrations two reactions and two sets of corresponding thermodynamic parameters have to be considered:



The thermal power generated upon the competitive ligand binding titration can be expressed as

$$P = \left(\Delta H_A \frac{d([MA])}{dt} + \Delta H_B \frac{d([MB])}{dt} \right) \cdot \left(V_0 + \frac{dV}{dt} t \right), \quad (5)$$

where dV/dt is the injection rate.

The total concentrations of the reacting species according to the mass balance principle are

$$[M_{tot}] = [M] + [MA] + [MB], \quad (6)$$

$$[A_{tot}] = [A] + [MA], \quad \text{and} \quad (7)$$

$$[B_{tot}] = [B] + [MB]. \quad (8)$$

The equilibrium concentrations of the two complexes can be derived by combining Eq. (7) or Eq. (8) with the equation for the corresponding binding constant:

$$[MA] = \frac{[M] \cdot [A_{tot}] K_A}{1 + [M] K_A} \quad \text{and} \quad (9)$$

$$[MB] = \frac{[M] \cdot [B_{tot}] K_B}{1 + [M] K_B}. \quad (10)$$

Substituting Eqs. (9) and (10) into Eq. (6) and collecting the like terms gives a cubic equation,

$$[M]^3 + a[M]^2 + b[M] + c = 0, \quad (11)$$

where the coefficients are

$$a = \frac{1}{K_A} + \frac{1}{K_B} + [A_{tot}] + [B_{tot}] - [M_{tot}],$$

$$b = \frac{[A_{tot}] - [M_{tot}]}{K_B} + \frac{[B_{tot}] - [M_{tot}]}{K_A} + \frac{1}{K_A K_B}, \quad \text{and}$$

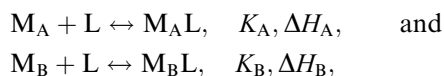
$$c = -\frac{[M_{tot}]}{K_A K_B}.$$

The only physically meaningful solution of Eq. (11) [20] gives the concentrations of the two complexes expressed through Eqs. (9) and (10).

To convert the calculated absolute concentrations into differential concentrations that are needed for cITC data analysis, $d[MA]/dt$ and $d[MB]/dt$ in Eq. (5), one needs to differentiate Eqs. (9) and (10). The analytical solution is complicated due to the extended sets of equations. For this reason we have calculated $d[MA]/dt$ and $d[MB]/dt$ numerically. The parameters K_A , K_B , ΔH_A , and ΔH_B can be calculated from a nonlinear regression of cITC data fitted to Eq. (5).

Binding of a ligand to a macromolecule with two independent sites

A macromolecule with two independent binding sites can be considered as two independent species competing for the same ligand. Two equilibrium reactions and two sets of thermodynamic parameters have to be considered,



where K_A and K_B are the constants for the binding of ligand L to sites A and B of the macromolecule,

respectively, and ΔH_A and ΔH_B are the corresponding enthalpies.

The thermal power generated upon continuous titration of a macromolecule with two independent sites can be expressed as

$$P = \left(\Delta H_A \frac{d([M_A L])}{dt} + \Delta H_B \frac{d([M_B L])}{dt} \right) \cdot \left(V_0 + \frac{dV}{dt} t \right). \quad (12)$$

The total concentration of the ligand according to the mass balance principle is

$$[L_{\text{tot}}] = [L] + [M_A L] + [M_B L]. \quad (13)$$

The equilibrium concentrations of the two complexes in Eq. (13) can be expressed through the equations for the corresponding binding constants as

$$[M_A L] = \frac{[L] \cdot [M_{\text{tot}}] K_A}{1 + [L] K_A} \quad \text{and} \quad (14)$$

$$[M_B L] = \frac{[L] \cdot [M_{\text{tot}}] K_B}{1 + [L] K_B}. \quad (15)$$

Substituting Eqs. (14) and (15) into Eq. (13) and collecting like terms gives a cubic equation,

$$[L]^3 + a[L]^2 + b[L] + c = 0, \quad (16)$$

where the coefficients are

$$a = \frac{1}{K_A} + \frac{1}{K_B} + 2 \cdot [M_{\text{tot}}] - [L_{\text{tot}}],$$

$$b = \frac{K_A + K_B}{K_A K_B} [M_{\text{tot}}] - \frac{K_A + K_B}{K_A K_B} [L_{\text{tot}}] + \frac{1}{K_A K_B}, \quad \text{and}$$

$$c = -\frac{[L_{\text{tot}}]}{K_A K_B}.$$

The only physically meaningful solution of Eq. (16) [20] gives the concentrations of the two complexes expressed through Eqs. (14) and (15).

To convert the calculated absolute concentrations into differential concentrations that are needed for cITC data analysis, $d[MA]/dt$ and $d[MB]/dt$ in Eq. (5), one needs to differentiate Eqs. (14) and (15). The analytical solution is complicated due to the extended sets of equations. For this reason we have calculated $d[M_A L]/dt$ and $d[M_B L]/dt$ numerically. The parameters K_A , K_B , ΔH_A , and ΔH_B can be calculated from a nonlinear regression of cITC data fitted to Eq. (12).

Matlab 6.5 software (The MathWorks, USA) was used to fit and to generate simulated ITC and cITC data. Fitting of the experimental and simulated data was done by iterative optimization of the parameters by a nonlinear least-square minimization according to the Marquardt–Levenberg algorithm [21].

Results and discussion

The thermodynamic analysis of the data from a cITC experiment is meaningful only if the titration is performed at quasi-equilibrium. This is achieved when three conditions are met. First, the rate of the continuous injection should be the limiting factor for the reaction taking place in the calorimetric vessel. This is the case for most of the protein–ligand binding processes where the reaction rate is within the range of a fraction of a second. The method is not suitable for studying binding reactions with slow kinetics. Second, the rate of addition of a reactant should be truly continuous. The step-motor that drives the injection pump supplied with the *type 1 calorimeter* sets the lower limits of the injection rate to around 0.013 $\mu\text{L/s}$ for the 250- μL and 0.026 $\mu\text{L/s}$ for the 500- μL Hamilton syringe. The injector used in the *type 2 calorimeter* system maintains the minimum injection rate of 0.135 $\mu\text{L/s}$ for a 100- μL Hamilton syringe and 0.32 $\mu\text{L/s}$ for a 250- μL Hamilton syringe. The oscillating character of the calorimetric signal at injection rates close to or below these values reflects the pulsating flow of the reactant from the syringe. Third, the mixing in the calorimetric vessel must be efficient to avoid the formation of laminar flow and concentration gradients within the vessel. Prior to the cITC experiments the mixing efficiency for the *type 1 calorimeter* was tested on the bench using a titration unit equipped with a glass vessel otherwise identical to the stainless steel vessel. This allowed visual examination of the solution in the vessel upon continuous addition of a colored component. It was found that the golden propeller stirrer provides efficient mixing after 2 s for 60 rpm and after 1 s for 120 rpm stirring speed. The injection rates used in these tests were in the range from 0.02 to 0.2 $\mu\text{L/s}$.

A paddle-type stirrer stirs the coin-shaped 1.36-ml total-fill calorimetric cell of the *type 2 calorimeter*. The calorimetric cell is permanently mounted into the instrument and, therefore, a visual examination of the stirring efficiency is not possible. According to the manufacturer it takes a few seconds until a solution in the cell becomes homogeneously mixed. The mixing efficiency can be improved by increasing the stirring speed. However, as stated in the manual, the short-term noise increases with stirring rate, in particular above 700 rpm. Therefore, the stirring speed in our experiments was not higher than 700 rpm.

Chemical steady state calibration of type 1 calorimeter

The *type 1 calorimeter* is a heat-flow calorimeter. This type of calorimeter has an inherent relatively slow response. However, the slow response can be dynamically corrected for by introduction of instrumental time constants. Normally time constants are evaluated from electrical calibration of the calorimetric vessel. In this

work we have also performed a chemical steady state calibration to obtain the time constants. This was achieved by continuous injection of BaCl_2 into the calorimetric vessel containing a large excess of 18-crown-6. Experimental conditions ensured constant nearly 100% binding of BaCl_2 throughout the titration. Therefore, a nearly steady state signal was obtained. The cooling part of the calorimetric curve was used to calculate the time

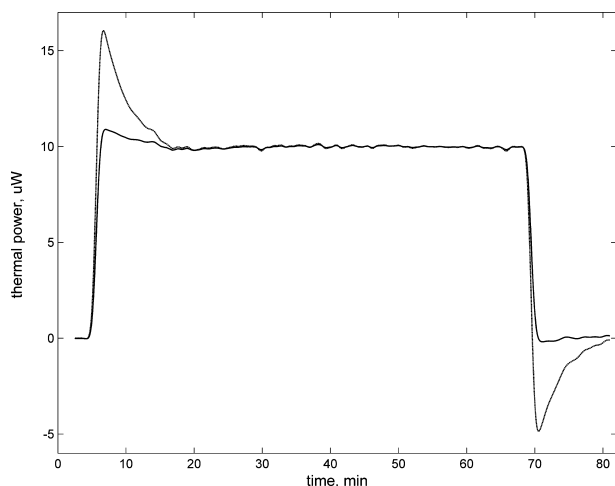


Fig. 1. Chemical steady state calibration; 5 mM BaCl_2 titrated at 21 nl/s into 900 μl 50 mM 18-crown-6.

constants of the calorimeter according to Laville [22]. It was found that one time constant was sufficient to describe the calorimetric signal with good accuracy. Fig. 1 shows that the quality of the dynamic correction of the raw calorimetric data for the instrumental time lag was significantly improved when the time constant obtained from the chemical calibration was used. The time constant obtained from the chemical calibration was chosen for the dynamic correction of the raw calorimetric data from the cITC experiments.

Low affinity 1:1 binding: BaCl_2 and 18-crown-6

The method of continuous titration was validated in application to the test reaction for titration calorimetry—binding of BaCl_2 to 18-crown-6 [14,15]. This reaction was performed in both types of calorimeters.

Type 1 calorimeter. Taking advantage of the highly flexible injection system of the *type 1* calorimeter, three injection rates were tested. This allowed us to optimize the setup of the continuous titration to the one that meets quasi-equilibrium conditions. Injection rates between 0.06 and 0.18 $\mu\text{l/s}$ were tested, resulting, respectively, in 50- to 12-min long titration experiments. As additional checks of mixing efficiency, two stirring speeds, 60 and 120 rpm, were used at each injection rate. Experiments at each injection rate and stirring speed

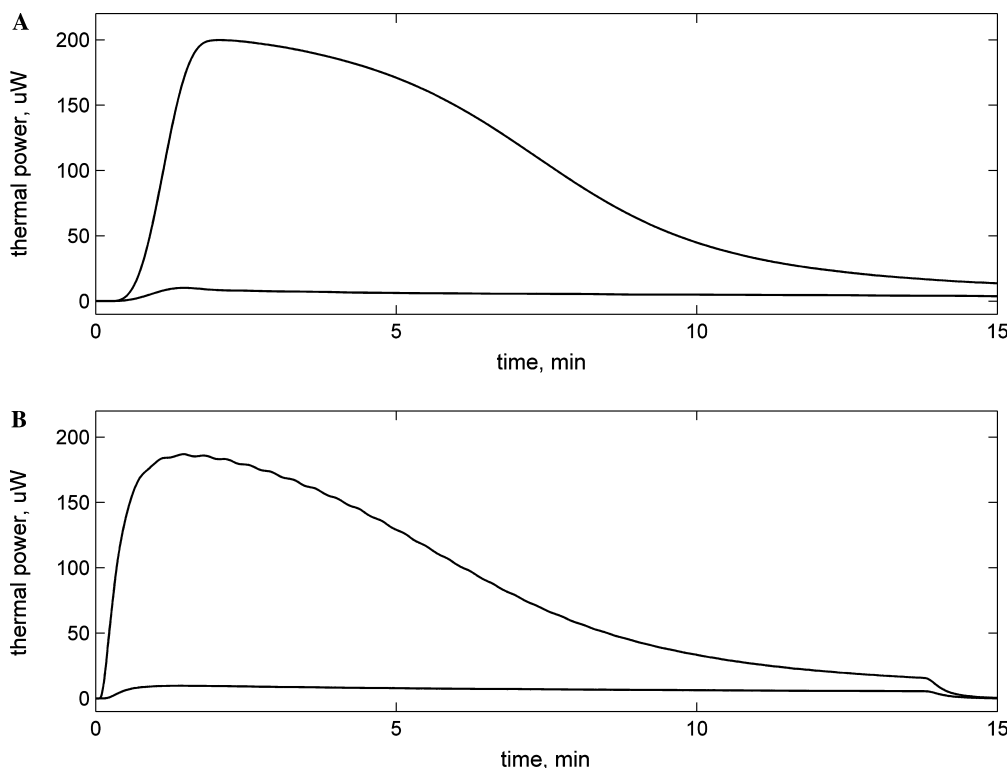


Fig. 2. Calorimetric data for the binding reaction of 18-crown-6 with BaCl_2 along with the corresponding BaCl_2 dilution data obtained by cITC at injection rate of 0.135 $\mu\text{l/s}$ in (A) *type 1* calorimeter and (B) *type 2* calorimeter. The concentration of BaCl_2 was 49.714 mM in both cases. Concentrations of 18-crown-6 were 3.1 mM for the *type 1* calorimeter and 1.66 mM for the *type 2* calorimeter. Measurements were carried out at 25 °C.

were repeated at least three times. Fig. 2A shows calorimetric data from continuous addition of BaCl_2 to 18-crown-6 and continuous addition of BaCl_2 to water at 0.135 $\mu\text{l/s}$ injection rate.

The thermal powers corrected for the effect of dilution were used to calculate the binding constants and the enthalpies of the reaction. Fig. 3A shows the best-fit curve from the nonlinear regression of the experimental data for the 0.135- $\mu\text{l/s}$ injection rate. The calculated values of K and ΔH are summarized in Table 1.

Thermodynamic parameters of the reaction obtained at 0.06 $\mu\text{l/s}$ injection rate are in a good agreement with the reference values from the stepwise titration [15]. The estimated precision of the binding constant is higher for cITC than for ITC. This is due to the increased number of experimental data points. The quality of the data for the reaction enthalpy is somewhat lower for the slowest injection rates due to the uncertainty in the baseline during a nearly 1-h-long injection. The precision in the estimated reaction enthalpies improves at higher

injection rates. However, the values of the binding constants become somewhat underestimated. Comparing the results obtained at the injection rate 0.06 $\mu\text{l/s}$ with the higher injection rates, the apparent binding constant decreases by 3.4% at the 0.135- $\mu\text{l/s}$ injection rate and by 8.8% at the 0.18- $\mu\text{l/s}$ injection rate. This effect is observed at both stirring speeds. However, the binding constant obtained at the 0.135- $\mu\text{l/s}$ injection rate is still within the limits of uncertainty of the reference value from the stepwise titration [15]. The observed effect is most probably the result of incomplete mixing, which would to some extent distort the shape of the titration curve, which is detrimental for accurate determination of K .

Type 2 calorimeter. Continuous titrations of 18-crown-6 with BaCl_2 were also performed on the *type 2 calorimeter*. Liu and Sturtevant [23] have extensively studied the thermodynamic parameters of the reaction between 18-crown-6 and BaCl_2 by ITC in this type of calorimeter ($K = 5140 \pm 40 \text{ M}^{-1}$, $\Delta H = -31.42 \text{ kJ/mol}$,

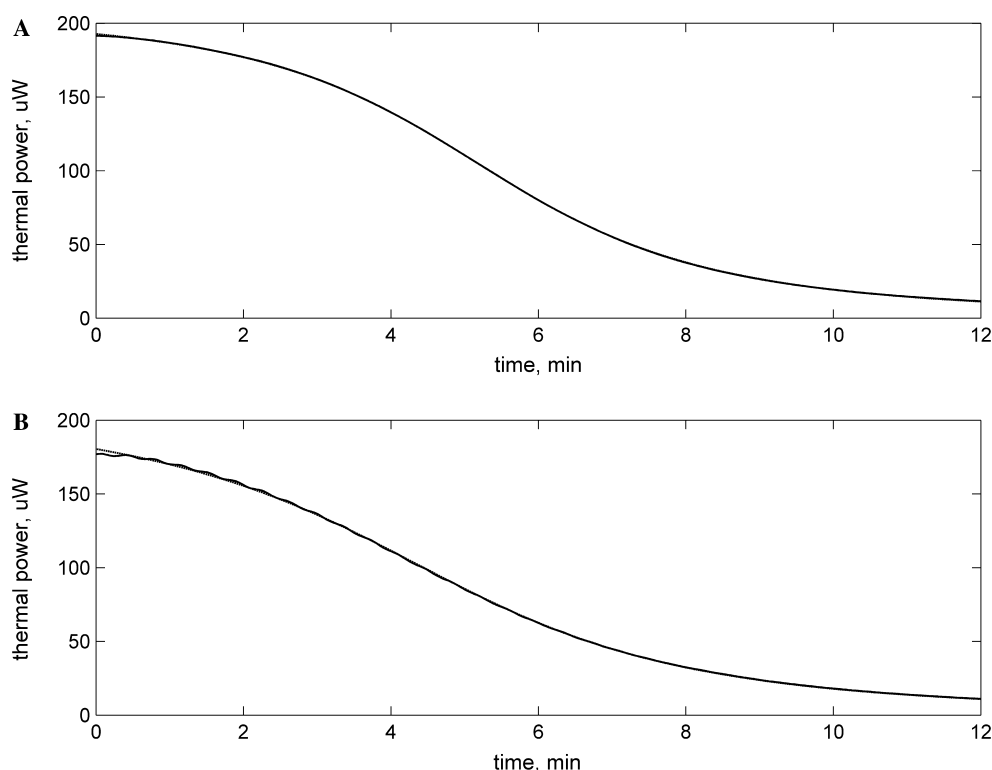


Fig. 3. Experimental thermal powers for the binding between BaCl_2 and 18-crown-6 corrected for dilution (solid line) and the data from the nonlinear regression to the 1:1 binding model (dashed line) in (A) *type 1 calorimeter* and (B) *type 2 calorimeter*. Measurements were carried out at 25 °C.

Table 1

Thermodynamic parameters of BaCl_2 binding to 18-crown-6 determined by cITC with *type 1* and *type 2 calorimeter* at 25 °C

	Type 1 calorimeter at 0.06 $\mu\text{l/s}$	Type 1 calorimeter at 0.135 $\mu\text{l/s}$	Type 1 calorimeter at 0.18 $\mu\text{l/s}$	Type 2 calorimeter 0.135 $\mu\text{l/s}$	Reference [15]
$K \text{ (M}^{-1}\text{)}$	5980 ± 100	5775 ± 14	5455 ± 42	4509 ± 256	5900 ± 200
$-\Delta H \text{ (kJ/mol)}$	31.45 ± 0.47	31.19 ± 0.04	31.70 ± 0.10	30.97 ± 0.15	31.42 ± 0.20

$n = 1.03$). The reported enthalpy of the reaction by Liu and Sturtevant [23] agrees very well with the value determined by ITC in a *type 1 calorimeter* by Briggner and Wadsö [15]. However, the number of active binding sites, n , used by Liu and Sturtevant as an additional

fitting parameter complicates direct comparison of the data. The binding constant determined in a *type 2 calorimeter* [23] is about 7% lower than the corresponding value for a *type 1 calorimeter* [15]. A plausible explanation for this would be that the binding reaction does not occur throughout the entire volume of the *type 2 calorimetric* vessel due to insufficient mixing. The mixing efficiency is the most important factor for a successful cITC experiment. Therefore, one would anticipate that the data from continuous titration in a *type 2 calorimeter* are especially prone to this kind of artifact.

This becomes apparent in the case of a continuous titration carried out at 400 rpm stirring speed (Fig. 4). The experimental binding curve deviates significantly from the calculated binding curve using the K value and ΔH value from Briggner and Wadsö [15]. The reaction enthalpy estimated from the integrated heat normalized with the number of moles of 18-crown-6 (Eq. (4)) is only 2% lower than the reference value. However, the corrupted shape of the binding isotherm makes the data unsuitable for calculation of a binding constant.

The results were significantly improved when the stirring speed was increased to 700 rpm (Fig. 2B). Fig. 3B shows the best-fit curve from the nonlinear regression of the experimental data obtained at stirring speed 700 rpm. The resulting thermodynamic parameters are summarized in Table 1.

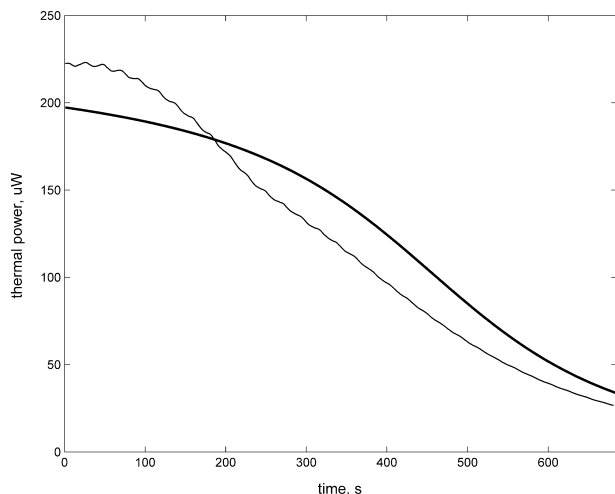


Fig. 4. Experimental (thin line) vs simulated (thick line) calorimetric curve for the continuous titration of 2.495 mM 18-crown-6 with 49.71 mM BaCl_2 in the *type 2 calorimeter*. The injection rate was 0.135 $\mu\text{l/s}$ and the stirring speed was set to 400 rpm. The experimental data have been corrected for the effect of dilution. Data refer to 25 $^{\circ}\text{C}$.

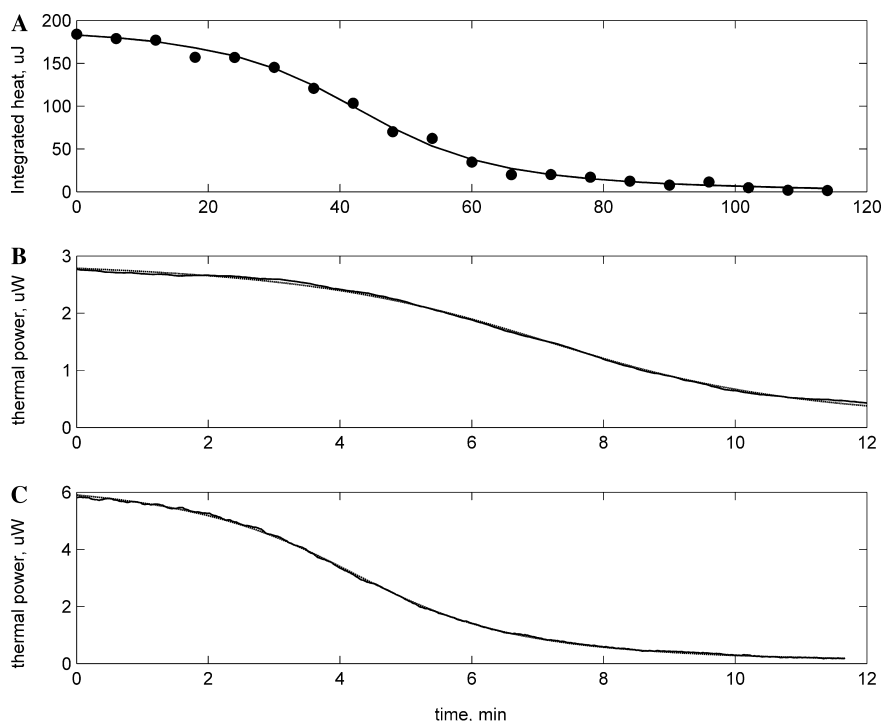


Fig. 5. Calorimetric data (solid line) along with the best-fit results (dashed line) for the binding of 2'CMP to RNase A. (A) Stepwise titration in *type 1 calorimeter*; 8- μl aliquots of 321 μM solution of 2'CMP were consecutively added to 23 μM solution of RNase A ($V_0 = 900 \mu\text{l}$); stirring speed was set to 60 rpm. (B) cITC measurement in *type 1 calorimeter*; 291 μM 2'CMP was continuously titrated into 23 μM RNase A ($V_0 = 900 \mu\text{l}$). (C) cITC measurement in *type 2 calorimeter*; 624 μM solution of 2'CMP was added at 0.135 $\mu\text{l/s}$ to the total-fill calorimetric cell containing 23 μM solution of RNase A. The experiment was carried out at 700 rpm stirring speed. The buffer composition, identical for all experiments, was 20 mM KAc, 20 mM KCl, pH 5.5. Measurements were carried out at 25 $^{\circ}\text{C}$.

The binding enthalpy obtained from three cITC experiments at 700 rpm stirring speed agrees well with the reference value. The binding constant is, however, underestimated by about 20%. The increased stirring speed does not entirely eliminate the effect of incomplete mixing and the reaction does not occur simultaneously throughout the working volume of the calorimetric vessel.

Biochemical 1:1 binding reaction: RNase A and 2’CMP

The binding of cytidine 2’-monophosphate (2’CMP) to RNase A was used as a test system to confirm that the cITC method can be applied on biochemical binding reactions. These systems have normally higher affinities, which means that lower concentrations are used in the experiments, leading to a lower calorimetric response.

The thermodynamic parameters of the reaction between 2’CMP and RNase A show strong concentration

dependence. According to Wiseman et al. [6], at lower concentrations of the protein and the ligand the apparent binding constant and the exothermicity of the enthalpy become larger. Therefore, low concentrations of the reagents and low salt content buffer were chosen to validate the cITC method.

Type 1 calorimeter. The data from an ITC experiment for the binding of 2’CMP to RNase A are shown in Fig. 5A. The mean value of the integrals of the peaks from the last eight injections (not included into the fit) was used to correct for the effect of dilution of 2’CMP. Spectroscopically determined active concentration of the protein was further verified by setting it as a variable parameter in the fit of the ITC data.

The injection rate for the cITC experiments was set to 0.135 µl/s and the stirring speed to 60 rpm. The experiment was repeated three times. A calorimetric curve from one of the cITC experiments and the calculated best-fit curve are shown in Fig. 5B. The mean of the

Table 2
Thermodynamic parameters for the binding of RNase A with 2’CMP

	ITC type 1 calorimeter	cITC type 1 calorimeter	cITC type 2 calorimeter
$K \text{ (M}^{-1}\text{)}$	$(0.852 \pm 0.080) \times 10^6$	$(0.865 \pm 0.010) \times 10^6$	$(0.826 \pm 0.028) \times 10^6$
$-\Delta H \text{ (kJ/mol)}$	75.45 ± 0.95	75.62 ± 0.20	76.85 ± 0.10

Injection rate for the cITC experiments was set to 0.135 µl/s. Stirring speeds were 60 and 700 rpm for *type 1* and *type 2* calorimeters, respectively. Data refer to 25 °C.

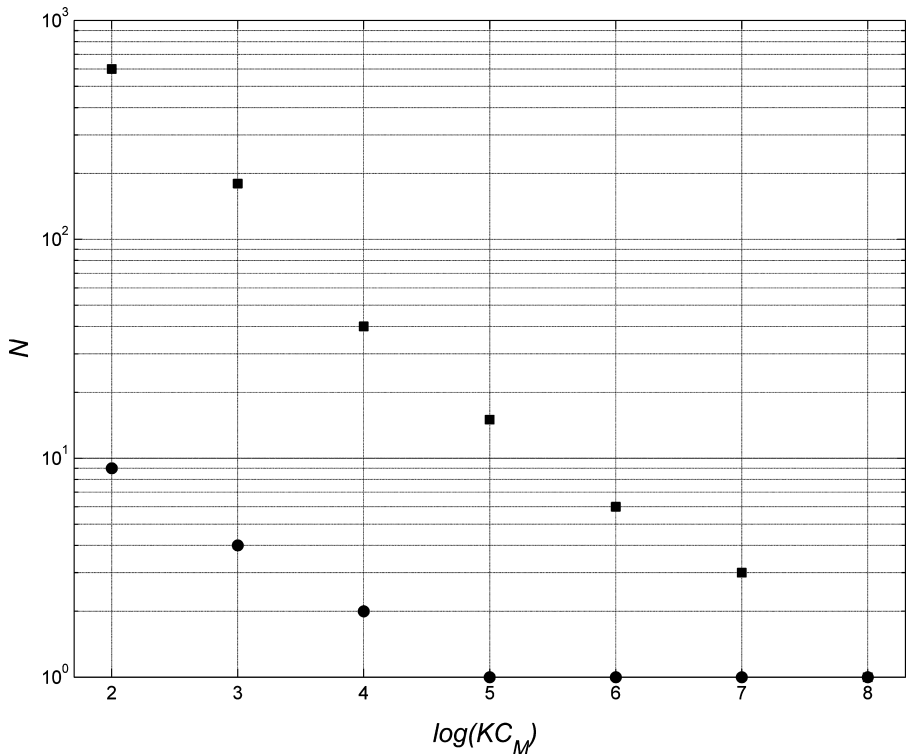


Fig. 6. Comparison of the number of experimental data points in the transition part of the 1:1 binding curve for the stepwise (circles) and continuous (squares) titrations as a function of the KC_M values. The following parameters were used in the simulations: $\Delta r = \Delta n_{L,tot}/n_{M,tot}$ was set to 0.1 for the stepwise and 0.0018 s⁻¹ for the continuous titration, $V_0 = 900 \mu\text{l}$. The number of injections for the stepwise titration was set to 30. For the continuous titration a 25-min-long injection at 0.18 µl/s was used.

calorimetric signal for the last few minutes of the continuous titration was used to correct for the contribution from heat of dilution. The heat of dilution contribution may also be added as a constant thermal power parameter in the fitting equation if the heat of dilution is assumed to be concentration independent at the concentration range of the experiment.

Thermodynamic parameters obtained from ITC and cITC using the *type 1 calorimeter* are in a good agreement (Table 2). The benefits of the cITC are a more than 10-fold reduction in experimental time and a 30-fold increase in the number of experimental data points, which improves the precision of the optimized thermodynamic parameters.

Type 2 calorimeter. The applicability of continuous titration to the high-sensitivity measurement range was tested in the *type 2 calorimeter* at 0.135 $\mu\text{l/s}$ injection rate and 700 rpm stirring speed. A calorimetric curve from a cITC experiment where 2'CMP is added to RNase A and the calculated best-fit curve are shown in Fig. 5C.

The heat of dilution correction was determined in a separate experiment. The calculated thermodynamic parameters are summarized in Table 2.

It can be concluded that continuous titration can be successfully applied also to the *type 2 calorimeter*. Taking into account strong nonideality effects reported for the binding of RNase A with 2'CMP, the thermodynamic parameters in Table 2 agree well with the values earlier reported by Wiseman et al. [6]. The reported values, $K = 1.0 \times 10^6 \text{ M}^{-1}$ and $\Delta H = -71 \text{ kJ/mol}$ at 25 °C, were obtained from ITC in a *type 2 calorimeter* at low concentration of RNase A in low-salt buffer, 45 μM RNase A in 50 mM potassium acetate, pH 5.5 [6]. These thermodynamic parameters are also close to the values calculated from ITC and cITC experiments in the *type 1 calorimeter*.

However, a direct comparison of the quality of the results obtained in the two calorimeters is difficult due to the possible nonideality effects. The experiments in the *type 2 calorimeter* were performed at concentrations of 2'CMP that were twice the concentrations used for the cITC experiments in the *type 1 calorimeter*. In addition, the K values and ΔH values obtained from the fit are highly dependent on the accuracy of the protein concentration and the quality of the dilution correction. The *type 2 calorimetric* cell is normally not dried before loading protein solution. Thus, the actual concentration in the cell is lower than expected. For this reason, the filling routine of the *type 2 calorimetric* cell is of importance.

Apparently, the reaction of RNase A with 2'CMP has to be used with caution as a test reaction. This is due to the nonideality effects and the reported strong dependence of the thermodynamic parameters on the type of cations in solution [24]. Presence of divalent cations in an insufficiently washed calorimetric vessel can dramatically change the binding thermodynamics.

Table 3

Parameters used for generating simulated cITC data and ITC data

Parameters	ITC	cITC
K_A (M^{-1})	1×10^7	1×10^7
ΔH_A (kJ/mol)	50	50
K_B (M^{-1})	1×10^5	1×10^5
ΔH_B (kJ/mol)	70	70
Endogenous ligand $[B_0]$ (μM)	5	5
Protein concentration in vessel $[M_0]$ (μM)	30	30
Ligand concentration in syringe $[A]$ (μM)	300	300
Initial vessel volume V_0 (μl)	900	900
Injection volume V (μl)	10	—
Injection rate (dV/dt) ($\mu\text{l/s}$)	—	0.18
Number of points	25	1200
Applied enthalpy noise (μJ)	4	—
Applied thermal power noise (nW)	—	40

Table 4

Thermodynamic parameters obtained from the fits of the simulated competition binding data to the different binding models

Model	ITC	cITC
1:1 Binding with a competing endogenous ligand present	$K_A = (1.09 \pm 0.79) \times 10^7 \text{ M}^{-1}$ $\Delta H_A = 50 \pm 26 \text{ kJ/mol}$ $K_B = (0.9 \pm 1.1) \times 10^5 \text{ M}^{-1}$ $\Delta H_B = 67 \pm 82 \text{ kJ/mol}$ $[B_0] = 5 \pm 7 \mu\text{M}$ std of the point = 5.5 μJ	$K_A = (1.00 \pm 0.35) \times 10^7 \text{ M}^{-1}$ $\Delta H_A = 49.6 \pm 0.7 \text{ kJ/mol}$ $K_B = (1.1 \pm 0.4) \times 10^5 \text{ M}^{-1}$ $\Delta H_B = 63 \pm 48 \text{ kJ/mol}$ $[B_0] = 5 \pm 3 \mu\text{M}$ std of the point = 42 nW
1:1 Binding	$K = (1.53 \pm 0.13) \times 10^6 \text{ M}^{-1}$ $\Delta H = 47.6 \pm 1.7 \text{ kJ/mol}$ std of the point = 8.6 μJ	$K = (4.38 \pm 0.15) \times 10^6$ $\Delta H = 45.30 \pm 0.11 \text{ kJ/mol}$ std of the point = 113 nW
2:1 Independent site	$K_A = (2.0 \pm 4.6) \times 10^6 \text{ M}^{-1}$ $\Delta H_A = 42 \pm 73 \text{ kJ/mol}$ $K_B = (2.0 \pm 5.6) \times 10^4 \text{ M}^{-1}$ $\Delta H_B = 39 \pm 110 \text{ kJ/mol}$ std of the point = 9.2 μJ	$K_A = (4.99 \pm 0.63) \times 10^6$ $\Delta H_A = 45.2 \pm 1.2 \text{ kJ/mol}$ $K_B = (0.50 \pm 0.28) \times 10^4$ $\Delta H_B = 40.0 \pm 18.6 \text{ kJ/mol}$ std of the point = 124 nW

Baseline noise added to the simulated data was 4 μJ for the stepwise titration and 40 nW for the continuous titration.

Dynamic range of binding affinities

One of the drawbacks of ITC is the relatively narrow range of attainable dissociation constants. In practice the range is approximately three orders of magnitude from a given concentration of the host molecule in the calorimetric vessel [6]. The ability to resolve the equilibrium constant with satisfactory statistical precision is related to the shape of the binding curve and the number of points in the region where the change in the degree of conversion to a complex is significant. In Fig. 6 the number of data points in the transition part of the binding curve has been plotted against the product between the equilibrium constant and the host molecule concentration, KC_M , for ITC and cITC. The plot represents data for the experimental conditions specified in the figure legend. In the simulations of the ITC titration the molar ratio between ligand and host molecule changed with 0.1 units per each addition of the ligand for ITC. For cITC this was 0.0018 for each point. This means that there was a 55.5-fold difference in data point density between the cITC and the ITC data.

It is obvious from Fig. 6 that the attainable equilibrium constant range for ITC is $1 \leq KC_M \leq 1000$. The increase in data density extends the upper limit of attainable equilibrium binding constant by three to four orders of magnitude. This means that an attainable equilibrium constant range for a cITC experiment is $1 \leq KC_M \leq 3 \times 10^6$. Therefore, the largest attainable equilibrium constant using cITC would be $K = 10^{11}–10^{12} \text{ M}^{-1}$. Today the highest equilibrium constant that is possible to determine by ITC in a sensitive calorimeter is of the order of $K = 10^8 \text{ M}^{-1}$.

Potential to discriminate between different binding models

The high-density data provided by cITC make it easier to differentiate between different binding models. To study the effect of high-density data we have generated computer-simulated ITC and cITC data. We assumed that the added ligand forms a 1:1 complex with the protein. To mimic the condition often encountered in protein binding studies, a competing endogenous ligand was present in the protein solution at a concentration of 16% of the protein concentration in the vessel. This means that the added ligand forms a 1:1 complex with the protein and that the ligand competes with another ligand at the same binding site. The simulated data were calculated from the parameters shown in Table 3. Random noise was added to the data, the maximum noise values were set to 40 nW for cITC and 4 μJ for ITC, which are typical for the performance of the calorimeters. The simulated data were analyzed applying three different binding models: a 1:1 binding model, a 2:1 independent site model, and a 1:1 binding model in the presence of a competing ligand. The results from the

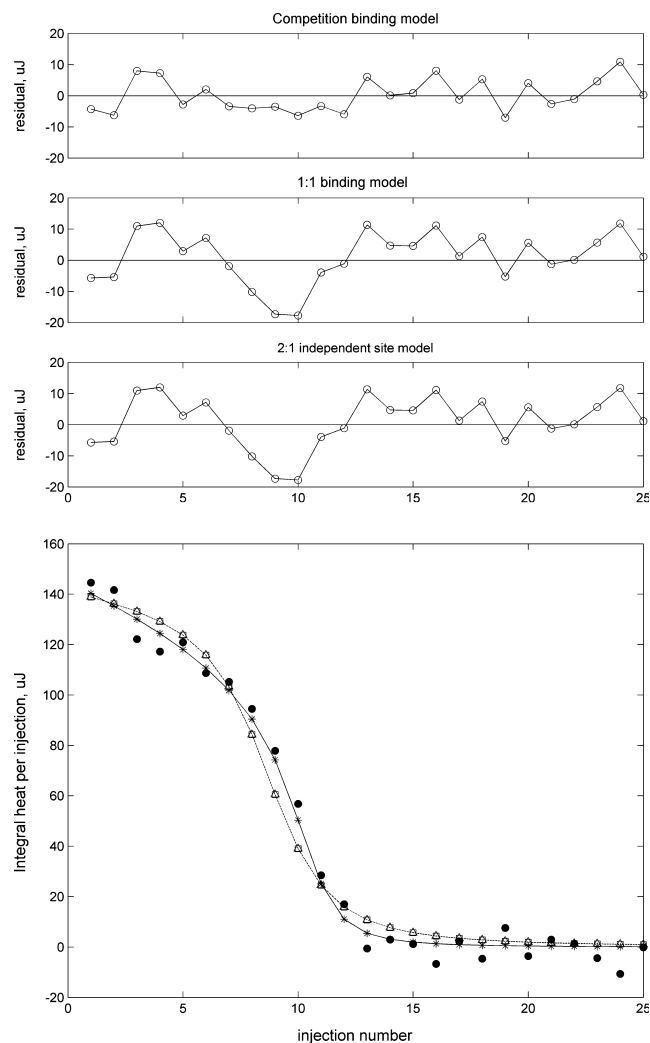


Fig. 7. (Bottom panel) Simulated binding curve for competition step-wise titration in the presence of an endogenous competing ligand (closed circles) and calculated results of the fit to the models: competition binding (asterisks and solid line); 1:1 binding (squares and dashed line); binding to a molecule with two independent sites (triangles and dashed line). (Top panels) Residual plots of the fits of the simulated competition binding ITC data to the different binding models.

fits for the three different models are shown in Table 4. The simulated and fitted curves along with the corresponding residuals are shown graphically in Fig. 7 for ITC and in Fig. 8 for cITC. The plots of the residuals show the benefit of cITC in comparison to ITC. The nonrandomly scattered residuals from the incorrect models are better identified for the simulated cITC data than for the simulated ITC data. The standard errors of point obtained for the incorrect models for the cITC fits were threefold larger than the random noise, while the correct model returned a standard error of point that is close to the random noise (Table 4). For the fits of the simulated ITC data the standard errors of point for the

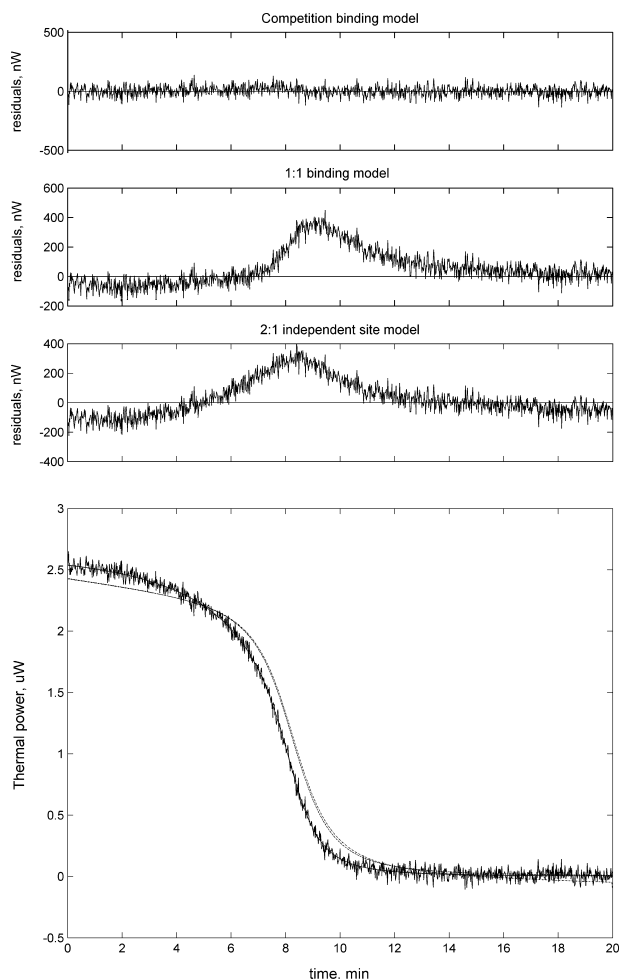


Fig. 8. (Bottom panel) Simulated binding curve for the competition continuous titration in the presence of an endogenous competing ligand and calculated curves from the fit to the models: competition binding (solid line); 1:1 binding (dashed line); binding to a molecule with two independent sites (dashed-dotted line). (Top panels) Residual plots of the fits of the simulated competition binding cITC data to the different binding models.

incorrect models did not differ much from the standard error of points of the correct model (Table 4). There are also striking differences between the cITC and the ITC in the quality of the fitted parameters for the correct model.

Conclusions

We believe that cITC can be a fast and precise tool for determining affinities and other thermodynamic properties. The cITC method shortens the experimental time by a factor of 10 compared to classical ITC and increases the number of data points 30-fold. The increase in data density significantly improves the quality of the fit and generates higher precisions in estimated thermodynamic parameters. With the high data density

we can better discriminate between different binding models. The range of affinities that can be calculated is increased from $1 \leq KC_M \leq 1000$ for ITC to $1 \leq KC_M \leq 3 \times 10^6$ for cITC. This means that the strongest attainable dissociation constant possible to resolve with cITC is on the order of 10 pM.

Acknowledgments

We thank Dr. Vildan Dincbas-Renqvist at KTH, Stockholm for the possibility to use the MCS ITC unit and for her kind assistance during the experiments.

References

- [1] J.S. Bardi, I. Luque, E. Freire, Structure based thermodynamic analysis of HIV-1 protease inhibitors, *Biochemistry* 36 (1997) 6588–6596.
- [2] E. Freire, K. Murphy, J.M. Sanchez-Ruiz, M. Galisteo, P. Privalov, The molecular basis of cooperativity in protein folding. Thermodynamic dissection of interdomain interactions in phosphoglycerate kinase, *Biochemistry* 31 (1992) 250–256.
- [3] J. Livingstone, R. Spolar, T. Record Jr., Contribution to the thermodynamics of protein folding from the reduction in water-accessible nonpolar surface area, *Biochemistry* 30 (1991) 4237.
- [4] R.B. Spokane, S.J. Gill, Titration microcalorimeter using nanomolar quantities of reactants, *Rev. Sci. Instrum.* 52 (1981) 1728–1733.
- [5] I.R. McKinnon, L. Fall, A. Parody-Morreale, S.J. Gill, A twin titration microcalorimeter for the study of biochemical reactions, *Anal. Biochem.* 139 (1984) 134–139.
- [6] T. Wiseman, S. Williston, J. Brandts, L.-N. Lin, Rapid measurement of binding constants and heats of binding using a new titration calorimeter, *Anal. Biochem.* 179 (1989) 131–137.
- [7] P. Bäckman, M. Bastos, D. Hallén, P. Lönnbro, I. Wadsö, Heat conduction calorimeters: time constants, sensitivity and fast titration experiments, *J. Biochem. Biophys. Methods* 28 (1994) 85–100.
- [8] R.L. Biltonen, N. Langerman, Microcalorimetry for biological chemistry: experimental design, data analysis, and interpretation, *Methods Enzymol.* 61 (1979) 287–318.
- [9] D. Hallén, Data treatment: considerations when applying binding reaction data to a model, *Pure Appl. Chem.* 65 (1993) 1527–1532.
- [10] F. Becker, Continuous titration calorimetry. I. Experimental methods and the titration calorimeter, *Chem. Ing. Tech.* 41 (1969) 1060–1068.
- [11] F. Becker, Continuous titration calorimetry. II. Applications, *Chem. Ing. Tech.* 41 (1969) 1105–11010.
- [12] A. Vacca, A. Sabatini, L. Bologni, A procedure for the calculation of enthalpy changes from continuous-titration calorimetric experiments, *J. Chem. Soc. Dalton Trans.* (1981) 1246–1250.
- [13] M. Barres, J.P. Dubes, R. Romanetti, H. Tachoire, C. Zahra, Determination of thermodynamic constants of solution equilibrium by conduction calorimetry and reactive flux. I. Description of the method, *Thermochim. Acta* 11 (1975) 235–246.
- [14] I. Wadsö, R.N. Goldberg, Standards in isothermal microcalorimetry, *Pure Appl. Chem.* 73 (2001) 1625–1639.
- [15] L.-E. Briggner, I. Wadsö, Test and calibration processes for microcalorimeters, with special reference to heat conduction

- instruments used with aqueous systems, *J. Biochem. Biophys. Methods* 22 (1991) 101–118.
- [16] C.N. Pace, F. Vajdos, L. Fee, G. Grimsley, T. Gray, How to measure and predict the molar absorption coefficient of a protein?, *Protein Sci.* 4 (1995) 2411–2423.
- [17] J. Suurkuusk, I. Wadsö, A multichannel microcalorimetry system, *Chem. Scripta* 20 (1982) 155–163.
- [18] M. Görman-Nordmark, J. Laynez, A. Schön, J. Suurkuusk, I. Wadsö, Design and testing of a new microcalorimetric vessel for use with living cellular systems and in titration experiments, *J. Biochem. Biophys. Methods* 10 (1984) 187–202.
- [19] B.W. Sigurskjold, Exact analysis of competition ligand binding by displacement isothermal titration calorimetry, *Anal. Biochem.* 277 (2000) 260–266.
- [20] Z.-X. Wang, An exact mathematical expression for describing competitive binding of two different ligands to a protein molecule, *FEBS Lett.* 360 (1995) 111–114.
- [21] P.R. Bevington, *Data Reduction and Error Analysis for Physical Sciences*, McGraw-Hill, New York, 1969.
- [22] G. Laville, Experimental calibration of the Calvet microcalorimeter, *Comp. Rend.* 240 (1955) 1195–1197.
- [23] Y. Liu, J.M. Sturtevant, Significant discrepancies between van't Hoff and calorimetric enthalpies. II, *Protein Sci.* 4 (1995) 2559–2561.
- [24] S.D. Spencer, O. Abdul, R.J. Schulingkamp, R.B. Raffa, Towards the design of the Rnase inhibitors: ion effects on the thermodynamics of binding of 2'CMP to Rnase A, *J. Pharm. Exp. Therapeut.* 301 (2002) 925–929.